

Development of a Lower Extremity Exoskeleton for Human Performance Enhancement

Xiaopeng Liu
School of Mech. & Prod. Engrg. (MPE)
Nanyang Technological University
Singapore 639798
Email: lxp@pmail.ntu.edu.sg

K. H. Low
School of MPE
Nanyang Technological University
Singapore 639798
Email: mkhlow@ntu.edu.sg

Hao Yong Yu
DSO National Laboratories
Defence Science Organization (DSO)
Singapore 118230
Email: yhaoyong@dso.org.sg

Abstract— Exoskeletons for human performance augmentation are controlled and wearable devices and machines that can increase the speed, strength, and endurance of the operator. So far most researchers focus on the upper limb exoskeletons. To help those who need to travel long distances by feet with heavy loads such as infantry soldiers, this paper presents a control principle of a lower extremity exoskeleton. An exoskeleton foot is designed to measure the human and the exoskeleton's ZMP. Using the measured human ZMP as the reference together with the human leg position signals, the exoskeleton's ZMP is modified by trunk compensation. Test prototypes and initial experiment results are also demonstrated.

I. INTRODUCTION

While research on humanoid robots has begun since many years ago, so far there are no robots can perform tasks in a wide range of fuzzy conditions preserving the same quality of performance as humans. Compared to human naturally developed algorithms with complex and highly specialized control methods, the artificial control algorithms that govern robots miss the flexibility. On the other hand, robots can easily perform some tasks human cannot do due to their physical limits such as lifting a heavy object. It seems therefore that combining these two entities, the human and the robot, into one integrated system under the control of the human, may lead to a solution that will benefit from the advantages offered by each sub system. Exoskeletons are such systems based on this principle.

Exoskeletons for human performance enhancement are controlled and wearable devices and machines that can increase the speed, strength, and endurance of the operator. The human provides control signals for the exoskeleton, while the exoskeleton actuators provide most of the power necessary for performing the task. The human applies a scaled-down force compared with the load carried by the exoskeleton.

Hardiman [1], developed by General Electric Corporation in the 1960's, was the first attempt at a man-amplifying exoskeleton. It was a 1,500-pound, 30-DOF, hydraulic and electric full body suit and was solved as a master-slave follower system. It was designed for amplification ratio of 25:1. It was bulky, unstable, and unsafe for the operator. Unsupported walking was not achieved. Later, Kazerooni [2], [3] developed an arm extender utilizing the

direct contact forces between the human and the machine measured by force sensors as the main command signal to the exoskeleton. Rosen *et al.* [4] synthesized the processed myoelectricity (EMG) signals as command signals with external-load/human-arm moment feedback to control an exoskeletal arm. Besides these, there are several other kinds of upper limb exoskeletons such as those in [5] and [6].

On lower extremity exoskeletons, most researchers paid their attention to developing walking aid systems for gait disorder persons or aged people. One of those systems is HAL (Hybrid Assistive Leg) [7], [8]. HAL can provide assist torques for the user's hip and knee joints according to the user's intention by using EMG signal as the primary command signal.

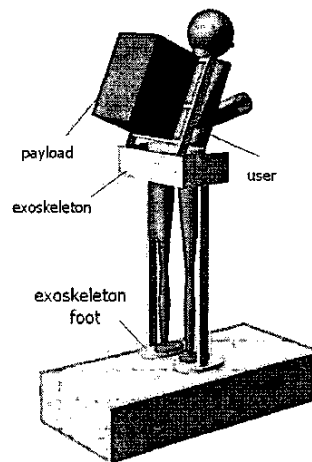


Fig. 1. Conceptual design of the exoskeleton

Different from HAL, the exoskeleton we are developing is to help those who need to travel long distances by feet with heavy loads such as infantry soldiers. Figure 1 shows a conceptual design. The exoskeleton affords the payload and keeps stability by the ground reaction force. Because the structure of the exoskeleton could be much firmer than human legs, it can carry heavy loads that a person cannot afford. With the help of the exoskeleton, the user can

carry more loads and walk longer before feeling tired if compared to those without the exoskeleton system. The system might provide soldiers, fire fighters, disaster relief workers, and other emergency personnel the ability to carry major loads such as food, weaponry, rescue equipment, and communications gear with minimal effort over any type of terrain for extended periods of time.

Next section will present the principle of the control of the exoskeleton. A lower extremity exoskeleton test fixture and some initial experiment results will be introduced in Section III. The conclusions and future work are presented in the last section.

II. PRINCIPLE OF THE CONTROL

A. Outline of the control principle

Biped gait can be divided into two phases: *single support phase* and *double support phase* [9].

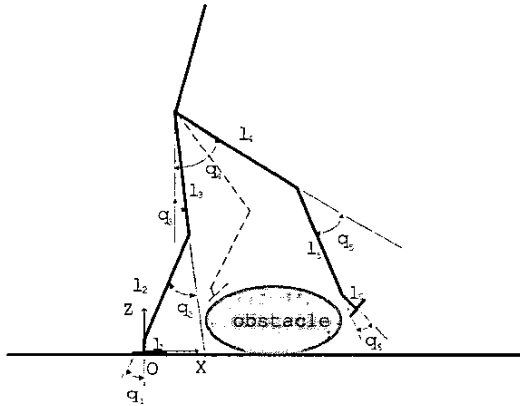


Fig. 2. Human in single support phase

1) *Leg trajectory control*: During the single support phase, the trajectory of the swinging foot determines the gait parameters such as step length, step height, etc. To make sure that the exoskeleton and the user can walk together, the trajectory of the exoskeleton's swing foot should trace that of the user in time. In the sagittal plane, the trajectory of the swinging foot can be described by

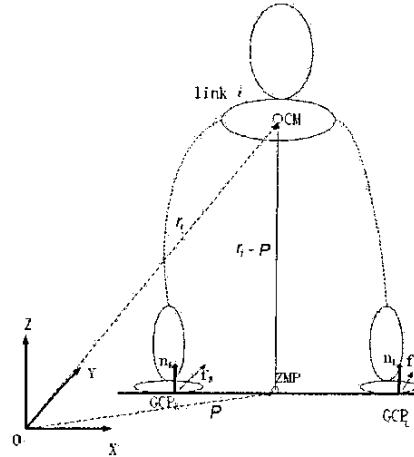
$$P_h(t) = \begin{bmatrix} x_h(t) \\ z_h(t) \end{bmatrix} = f(l_1, l_2, \dots, l_6; q_1(t), q_2(t), \dots, q_6(t)) \quad (1)$$

where l_i is the length of link i , and $q_i(t)$ is the trajectory of joint i . The lengths of the user's leg can be measured, and the angle of joints can be recorded by sensors such as encoders. Thus the position of the user's swing foot at each time interval can be calculated online to command the exoskeleton's swinging foot. To simplify the control, the length of the exoskeleton's leg will be designed to be adjustable. When the user wears the exoskeleton, the length will be adjusted to be the same as the user leg, then only the angles need to be controlled during the walking.

2) *ZMP control*: The Zero Moment Point (ZMP) [10] is defined as the point on the ground at which the net moment of the inertial forces and the gravity forces has no component along the horizontal axes. For the kinematic chain shown in Figure 3, the ZMP condition can be represented as:

$$\sum_{i=1}^n (m_i(\mathbf{r}_i - \mathbf{P}) \times (-\ddot{\mathbf{r}}_i + \mathbf{g})) - \mathbf{I}_i \alpha_i - \omega_i \times \mathbf{I}_i \omega_i = (0, 0, M_z) \quad (2)$$

where \mathbf{r}_i and \mathbf{P} are as defined in Figure 3, n is the number of links in the chain, m_i and \mathbf{I}_i are respectively, the mass and moment of inertia of link i , ω_i and α_i are, respectively, the angular velocity and angular acceleration of link i , and \mathbf{g} is the acceleration due to gravity. Also, M_z is the z component of the moment at ZMP (its value is immaterial for the computation of the ZMP). The coordinates of the ZMP can be obtained by solving this equation for the x and y components of \mathbf{P} .



CM stands for center of mass of link i .

Fig. 3. Definition of ZMP for a kinematic chain.

Another concept is the Ground Contact Point (GCP) [11], which is defined as the point on the foot through which a resultant reaction force and a reaction moment, orthogonal to the ground surface, act.

The gait is balanced when and only when the ZMP trajectory remains within the support area. In the single-support phase, the support polygon is identical to the foot surface. In the double support phase, the support area is defined by the convex hulls of the two supporting feet.

In a stable gait, during the single support phase, the GCP of the supporting foot is also the ZMP of the whole biped; during the double support phase, the relationship between the ZMP and the GCP is described by

$$X_p = \frac{f_{Lz} X_L + f_{Rz} X_R}{f_{Lz} + f_{Rz}}, \quad Y_p = \frac{f_{Lz} Y_L + f_{Rz} Y_R}{f_{Lz} + f_{Rz}} \quad (3)$$

where

- $ZMP = (X_p, Y_p, Z_p)$: ZMP of the whole biped.
- $GCP_L = (X_L, Y_L, Z_L)$: GCP of the left foot.
- $GCP_R = (X_R, Y_R, Z_R)$: GCP of the right foot.
- $f_L = (f_{Lx}, f_{Ly}, f_{Lz})$: ground reaction force at GCP_L .
- $f_R = (f_{Rx}, f_{Ry}, f_{Rz})$: ground reaction force at GCP_R .

If the ZMP of the exoskeleton can remain within the support area, it means that the exoskeleton can keep the stability only by using the ground reaction force without adding any force to the user. In other words, the user will not feel any extra burden from the exoskeleton.

As can be concluded from the above discussion, the exoskeleton should be controlled to satisfy the two requirements:

- The swing foot of the exoskeleton should closely trace that of the user in time.
- The ZMP of the exoskeleton should remain in support area.

B. Foot design

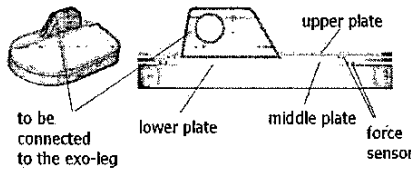


Fig. 4. Design of the exoskeleton foot

To control the ZMP of the exoskeleton, a footpad is designed as shown in Figure 4. The human foot will be on the upper plate, and the exoskeleton leg will be connected to the middle plate. There are four force sensors between the upper plate and middle plate, the middle plate and lower plate, respectively. The sensors are distributed as shown in Figure 5.

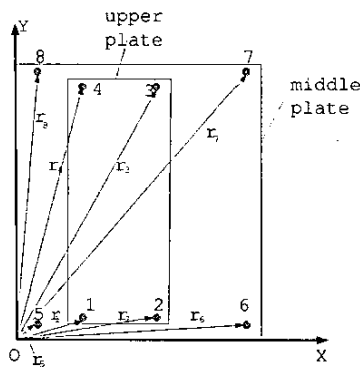


Fig. 5. Distribution of the sensors

During the single support phase, Sensors 1-4 measure the ground reaction force under the human foot, and the

ZMP coordinates of the human in the foot local coordinate frame can be calculated according to

$$ZMP_h = \frac{\sum_{i=1}^4 F_i r_i}{\sum_{i=1}^4 F_i} \quad (4)$$

where F_i is the force measured by sensor i at the distance from O , r_i , as defined in Figure 5. Sensors 5-8 measure the ground reaction force under the whole system (the human plus the exoskeleton). Similarly, the ZMP of the whole system can be calculated by

$$ZMP_w = \frac{\sum_{i=5}^8 F_i r_i}{\sum_{i=5}^8 F_i} \quad (5)$$

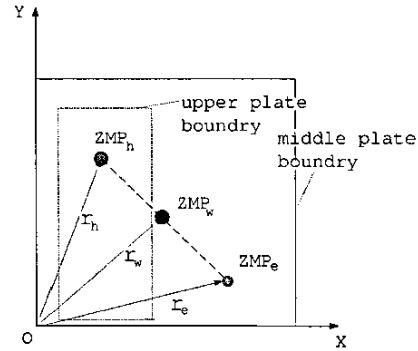


Fig. 6. Relationship between the human ZMP and the exoskeleton's ZMP

The ZMP of the exoskeleton is on the radial from the human ZMP to the whole system's ZMP, and its position can be obtained from the equation given by

$$ZMP_e = \frac{\sum_{i=1}^4 F_i (r_w - r_h)}{\sum_{i=5}^8 F_i - \sum_{i=1}^4 F_i} + r_w \quad (6)$$

in which r_h and r_w , as shown in Figure 6, are the coordinates of the human ZMP and the ZMP of the whole system, respectively.

During the double support phase, instead of the ZMPs, GCPs of each foot are obtained from Eqs. (4)-(6). By substituting those GCPs of the human and the exoskeleton into Eq. (3), respectively, ZMP of the human and that of the exoskeleton can be obtained accordingly.

Using the measured human ZMP as the reference, the desired ZMP of the exoskeleton can be chosen according to the following criterions:

- During the single support phase, the desired ZMP of the exoskeleton should be in the support foot area.
- During the double support phase, the human ZMP shifts from the hind foot to the former foot, the desired ZMP of the exoskeleton could be in the area between the two feet, but not too far from the measured human ZMP.
- At the end of the double support phase, when the human ZMP enters his/her former foot area, the desired ZMP of the exoskeleton should also enter the exoskeleton's former foot area.

C. Trunk compensation

If the actual (measured) ZMP of the exoskeleton differs from the desired ZMP, trunk compensation will be applied to shift the actual ZMP to an appropriate position.

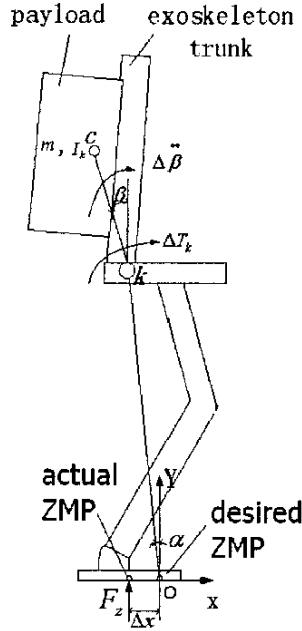


Fig. 7. Adjusting ZMP by trunk compensation

Without losing any generality, only motion in the sagittal plane, during single support phase is discussed here, and the trunk compensation in the frontal plane or during double support phase is performed in the similar way.

As shown in Figure 7, the actual ZMP differs from the desired ZMP in the direction of X axis by Δx . And the ground reaction force acts on the exoskeleton is F_z , which can be derived from $F_z = \sum_{i=5}^8 F_i - \sum_{i=1}^4 F_i$. An assumption introduced for the purpose of simplicity is that the action at the trunk joint will not cause a change in the motion at any other joint. In other words, the servo systems are supposed to be sufficiently stiff. Under this assumption, the system will behave as if it was composed of two rigid links connected at trunk joint k , as presented in Figure 7. The payload and the exoskeleton trunk are considered as an upper part of total mass m and inertia moment I_k for the axis of joint k . Point c is the mass center of the upper part, and the distance from c to k is denoted by l_1 . The lower part, representing the sum of all the links below the trunk joint k including the other leg that is not drawn in the figure, is also considered as a rigid body, which is standing on the ground surface and does not move. The distance from O to k is denoted by l_2 . Note that ΔT_k stands for the correctional additional actuator torque, applied at joint k .

Next, the following equations are derived:

$$\Delta T_k = I_k \Delta \ddot{\beta} \quad (7)$$

$$F_z \Delta x = \Delta T_k + ml_1 \Delta \dot{\beta} l_2 (\cos \beta \cos \alpha + \sin \beta \sin \alpha) + ml_1 \Delta \beta (\dot{\beta} + 2\Delta \dot{\beta}) l_2 (\cos \beta \sin \alpha + \sin \beta \cos \alpha) \quad (8)$$

Assuming that the additional torque ΔT_k will cause change in acceleration of the upper part $\Delta \ddot{\beta}$, while velocities will not change due to the action of ΔT_k , $\Delta \dot{\beta} \approx 0$. Equation (8) can then be simplified to

$$F_z \Delta x = \Delta T_k + ml_1 \Delta \ddot{\beta} l_2 (\cos \beta \cos \alpha + \sin \beta \sin \alpha) \quad (9)$$

By virtue of Eq. (7), we have

$$\Delta \ddot{\beta} = \frac{\Delta T_k}{I_k} \quad (10)$$

Substituting Eq. (10) into Eq. (8), we obtain

$$\Delta T_k = \frac{F_z \Delta x}{1 + \frac{ml_1 l_2 (\cos \beta \cos \alpha + \sin \beta \sin \alpha)}{I_k}} \quad (11)$$

Taking into account that ΔT_k is derived by introducing certain simplifications, an additional feedback gain K_{zmp} is introduced into Eq. (11). Thus, Eq. (11) becomes

$$\Delta T_k = K_{zmp} \cdot \frac{F_z \Delta x}{1 + \frac{ml_1 l_2 (\cos \beta \cos \alpha + \sin \beta \sin \alpha)}{I_k}} \quad (12)$$

where K_{zmp} can be decided by the feedback in the actual walking. Equation (12) shows how to drive the actual ZMP towards the desired ZMP by controlling the torque output of the trunk joint.

III. TEST PROTOTYPES AND INITIAL EXPERIMENTS

A. Exoskeleton foot

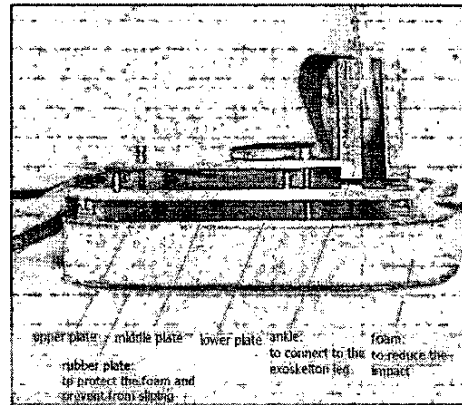


Fig. 8. The exoskeleton foot

The fabricated exoskeleton foot is shown in Figure 8. Besides the three plates and sensors described above, foam is added under the lower plate to reduce the transmission of impact forces. Furthermore, it acts as a mechanical lowpass filter that prevents the vibration of leg compliance control [12]. The sensors employed are Flexiforce sensor [13] and their coordinates in the foot coordinate frame are listed in Table I.

TABLE I
COORDINATES OF THE SENSORS

(X, Y) (mm)	Sensor 1	Sensor 2	Sensor 3	Sensor 4
	(0, 0)	(80, 0)	(80, 200)	(0, 200)
	Sensor 5	Sensor 6	Sensor 7	Sensor 8
	(-11, -11)	(131, -11)	(131, 210)	(-11, 210)

B. Test fixture

As shown in Figure 9, a test fixture has been fabricated to provide information that will be used to build a formal wearable lower body exoskeleton.

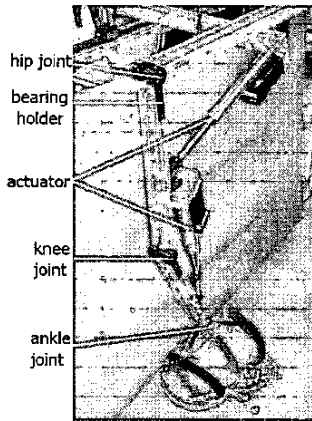


Fig. 9. The test fixture

Standard industrial components such as shaft supports, aluminum profiles, etc. are used to minimize machining. To suit different human leg lengths, the length between the hip joint and knee joint as well as that between the knee joint and the ankle joint are changeable by adjusting the position of the bearing holder on the aluminum profile.

C. Initial experiments

Experiments of controlling the exoskeleton's leg using the position signals measured from human leg have been performed. As shown in Figure 10(a), encoders are attached to the human joints to measure the human leg movements and the exoskeleton leg is controlled to perform the similar movements. Figures 10(b) and 10(c) are two snaps of the gait. Figure 10(b) shows the exoskeleton leg in swinging phase while Figure 10(c) shows its support phase.

During the procedure, the ground reaction force under the foot and the ZMP trajectories are recorded (see Figure 11) for further analysis and study. Figure 12 shows the signal flow during the experiment.

One problem can be seen from Figure 10 is that the encoder's size causes a big displacement between the exoskeleton's leg and human leg. Hence in the future version, the encoders will be replaced with goniometers [14]. The units have a telescopic endblock that compensates for changes in distance between the two mounting points as the limb moves. The gauge mechanism also allows for accurate measurement of polycentric joints.

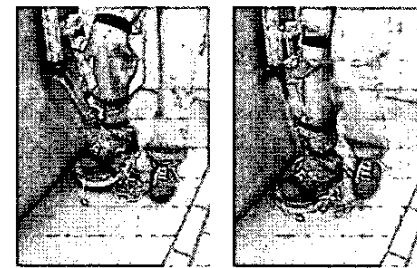
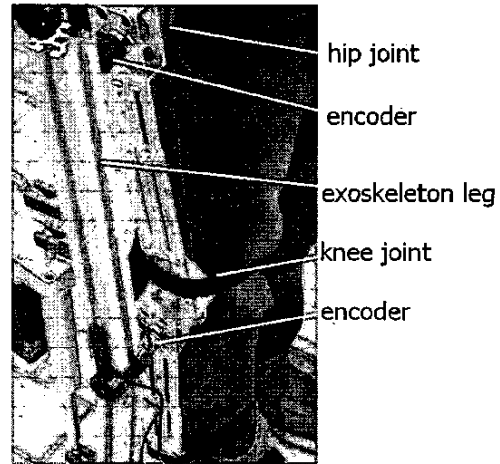


Fig. 10. Initial experiments

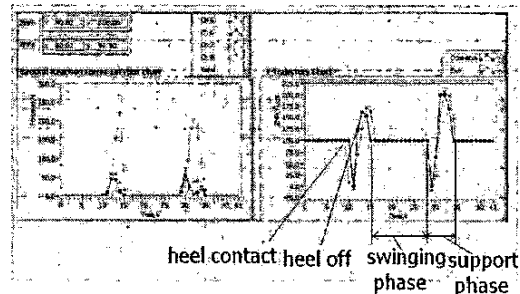


Fig. 11. Recorded ground reaction force and ZMP

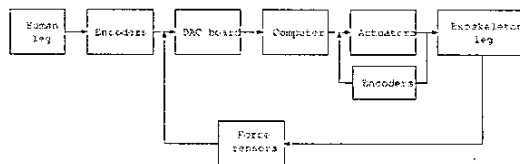


Fig. 12. System component and signal flow

D. Full version of the lower exoskeleton

The full version of the lower extremity exoskeleton (see Figure 13) is being developed, and further experiments will be performed.

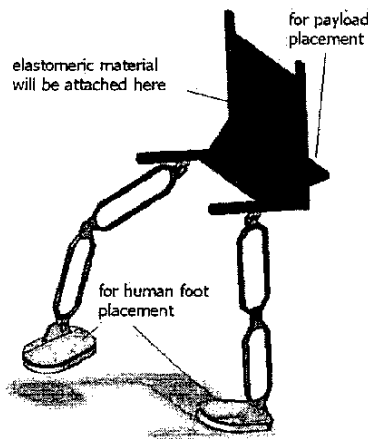


Fig. 13. The structure of the full lower extremity exoskeleton

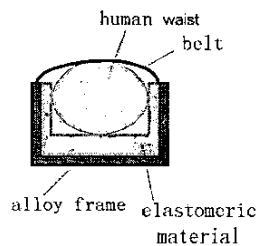


Fig. 14. Topview of the waist attachment

By observing typical human joints' trajectories it is noted that the motion range is much greater in sagittal plane than in other planes [15]. Also, during walking most movements happen in the sagittal plane. Hence, at the first stage, only the degrees of freedoms (DOF) in the sagittal plane are actuated (each one at the trunk, hip, knee and ankle, respectively). In the future, more DOFs may be added. The exoskeleton will be attached to the human at the feet and the waist. At the waist, between the alloy frame of the exoskeleton and the human is filled with elastomeric material, and a belt will fix them together, as shown in Figure 14. The side of the exoskeleton's trunk that is near to human trunk will also be enclosed with elastomeric material in order not to harm the user.

IV. CONCLUSIONS AND FUTURE WORK

This paper has presented a principle of a lower extremity exoskeleton, which is being developed to help those who need to travel long distances by feet with heavy loads. The leg trajectories of the exoskeleton are determined by

position signals measured from the human legs. The desired ZMP of the exoskeleton is chosen by using the measured human ZMP as the reference. The trunk compensation is then used to adjust the ZMP. Test prototypes and initial experiments have been demonstrated. The full version of the exoskeleton is being constructed and further experiments will be performed.

ACKNOWLEDGEMENTS

The authors would like to thank Ms. Wang-Yong Koh and Mr. Chin-Pang Chan for their assistance in programming and experiments. This research is supported by Research Grant MINDEF-NTU/02/01, a grant from the Ministry of Defence of Singapore. Robotics Research Center of Nanyang Technological University provides technical helps, space and facilities.

REFERENCES

- [1] M. Vukobratović, B. Borovac, D. Surla and D. Stokić, *Biped Locomotion: dynamics, stability, control, and application*, Springer-Verlag, Berlin, 1990.
- [2] H. Kazerooni, "Extender: a case study for human-robot interaction via transfer of power and information signals," *Proceedings of 2nd IEEE International Workshop on Robot and Human Communication*, pp. 10-20, 1993.
- [3] H. Kazerooni, "Human power extender: an example of human-machine interaction via the transfer of power and information signals," *1998 5th International Workshop on Advanced Motion Control*, pp. 565-572, 1998.
- [4] J. Rosen, M. Brand, M. B. Fuchs, and M. Arcan, "A myosignal-based powered exoskeleton system," *IEEE Transactions on Systems, Man and Cybernetics*, Part A, vol. 31, no. 3, pp. 210-222, 2001.
- [5] M. Bergamasco, B. Allotta, L. Bosio, L. Ferretti, G. Parrini, G. M. Prisco, F. Salsedo, and G. Sartini, "An arm exoskeleton system for teleoperation and virtual environments applications," *IEEE International Conference on Robotics and Automation*, vol. 2, pp. 1449-1454, 1994.
- [6] Homepage of the *Sarcos Online*, <http://www.sarcos.com>, June, 2004.
- [7] K. Kasaoka and Y. Sankai, "Predictive control estimating operators intention for stepping-up motion by exoskeleton type power assist system HAL," *Proceedings of IEEE/RSJ International Conference on Intelligent Robots and Systems*, pp. 1578-1583, 2001.
- [8] H. Kawamoto and Y. Sankai, "Comfortable power assist control method for walking aid by HAL-3," *Proceedings of IEEE International Conference on Systems, Man and Cybernetics*, vol. 4, 6 pages, 2002.
- [9] M. W. Whittle, *Gait analysis: an introduction*, Butterworth-Heinemann, Oxford, 1991.
- [10] M. Vukobratović and D. Juricic, "Contribution to the Synthesis of Biped Gait," *IEEE Transactions on Bio-Medical Engineering*, BME-16, No.1, pp. 1-6, 1969.
- [11] A. Dasgupta and Y. Nakamura, "Making feasible walking motion of humanoid robots from human motion capture data," *Proceedings of IEEE International Conference on Robotics and Automation*, vol. 2, pp. 1044-1049, 1999.
- [12] K. H. Low and Aiqiang Yang, "Design and foot contact of a leg mechanism with a flexible gear system," *Proceedings of 2003 IEEE International Conference on Robotics and Automation*, vol. 1, pp. 324-329, 2003.
- [13] Homepage of the *Flexiforce*, <http://www.tekscan.com/flexiforce.html>, June, 2004.
- [14] Homepage of the *BIOPAC*, http://biopac.com/fr_prod.htm, Jan, 2004.
- [15] S. Marchese, G. Muscato, and G. S. Virk, "Dynamically stable trajectory synthesis for a biped robot during the single-support phase," *Proceedings of IEEE/ASME International Conference on Advanced Intelligent Mechatronics*, vol. 2, pp. 953-958, 2001.